Nuclear Instruments and Methods in Physics Research A277 (1989) 176–186
North-Holland, Amsterdam

EXPERIMENTAL STUDY OF ELECTRON–HADRON SEPARATION IN CALORIMETERS USING SILICON DIODES

A. DWURAŹNY and W. KRUPINSKI

Institute of Nuclear Physics, Cracow, Poland

G. BARBAGLI and P.G. PELFER

Dipartimento di Fisica dell 'Università and INFN, Florence, Italy

D.G. CASSEL *, R. KLANNER, U. KÖTZ and W. KOCH

Deutsches Elektronen-Synchrotron DESY, Hamburg, FRG

J. TENGELER

II. Institut für Experimentalphysik der Universität Hamburg, Hamburg, FRG

N. WAINER

Weizmann Institute, Rehovot, Israel

The ZEUS group plans to install planes of large-area silicon diodes in depleted-uranium–scintillator calorimeters to separate electrons from hadrons in jets. This method was tested at 3, 5 and 9 GeV at CERN. Arrays of diodes were studied at depths between about 1 and 9 radiation lengths in a lead–scintillator calorimeter and in a simulated calorimeter consisting of depleted uranium and lucite. The e–h separation efficiency was measured for one and two planes of diodes as a function of depth in the calorimeter. A hadron misidentification of 2% at an electron efficiency of 90% was obtained with one plane of diodes. Addition of a second plane of diodes reduced the hadron misidentification to 0.3% with an electron efficiency of 90%. These results demonstrate that silicon diodes are excellent devices for e–h separation in a calorimeter.

1. Introduction

Separation of hadrons and electrons is crucial for experiments at the electron–proton storage ring, HERA, under construction at DESY. Even the simplest and most basic experiments must distinguish between charged current and neutral current events, for which it is necessary to determine if any one of the high-energy particles produced in the event was an electron.

The ZEUS Collaboration [1] at HERA is constructing high-resolution hermetic calorimeters built from depleted uranium, read out with scintillators, wavelength shifters and photomultipliers. The calorimeters are optimized for the best possible hadron energy resolution, which at the present understanding of hadron calorimetry has led to the choice of scintillator for the active medium. The calorimeters are segmented longitudinally into an electromagnetic section (25 radiation lengths, 1 interaction length) and two hadronic calorimeters (3 interaction lengths each). Separation of *isolated* electrons (e) from hadrons (h) by comparing the energy deposited in the electromagnetic and hadronic sections is relatively straightforward in these calorimeters. This technique of using differences in the longitudinal development of electron and hadron showers for e–h separation is a powerful tool [2–4].

Electrons within hadron jets pose a special problem if scintillator is used for the active medium, since small segmentation is difficult to achieve without dead space. A highly segmented detector measuring the number of charged particles near the maximum of the electromagnetic shower can solve this problem.

Semiconductor detectors (silicon diodes) are an almost ideal solution because of the following properties:
- excellent $\mathrm{d}E/\mathrm{d}x$ resolution and large dynamic range, limited in practice by the readout electronics;
- little material, compact and flexible design in almost any desired size and shape without bulky frames or enclosures;

* On sabbatical leave from Cornell University, Ithaca, NY, USA.

0168-9002/89/$03.50

- operation at low power with safe bias voltages, at room temperature and unaffected by magnetic fields;
- no flammable gases for their operation.

Possible problems for these detectors are:

- limitations from radiation damage;
- large capacitance and thus large electronics noise and difficulties to exploit the intrinsic speed of the detector.

Large semiconductor detectors capable of detecting minimum ionizing particles first found major use in elementary particle physics as vertex detectors [5]. Recently, large-area semiconductor detectors have been developed for use as the active medium in calorimeters [6], which is more closely related to the application discussed here. The properties listed above indicate that semiconductor detectors should be very useful for e–h separation in calorimeters. This article describes the results of an experimental study of e–h separation using silicon detectors in the energy range of 3–10 GeV. Extension of this work to energies up to 100 GeV will be the topic of a forthcoming publication.

2. The diodes, beam and data taking

The experimental test used four planes of silicon diodes that were inserted in a lead–scintillator calorimeter or a simulated depleted-uranium calorimeter with Lucite used instead of scintillator. The diodes and their geometrical arrangements are illustrated in fig. 1 and described in table 1. The Hamamatsu [7] diodes are strip detectors with 56 strips, each 0.5×28 mm^2. Groups of seven strips were connected together to make diodes that were 3.5×28 mm^2. The Hamamatsu, Micron [8] and Ansaldo [9] diodes were standard commercial-quality diodes. The diodes from the T.U. München has been rejected from normal production due to increased dark current. In the results in this article the signals of all the Hamamatsu diodes and of nine of each of the other types of diodes were added in software to simulate diodes covering an area of approximately 30×30 mm^2.

The lead calorimeter with scintillator and wavelength shifter readout is illustrated in fig. 2, and fig. 3 shows the simulated calorimeter made of depleted uranium

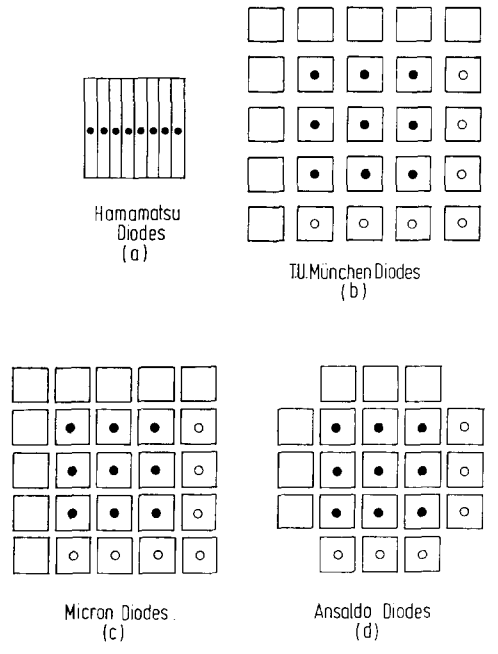

Fig. 1. The arrays of diodes used in the test. All strips of the Hamamatsu diodes were read out and used in this analysis. For the T.U. München, Micron and Ansaldo diodes, the diodes marked with ○ or ● were read out, and the nine diodes marked with ● were used in the analysis described in this article.

(DU) and Lucite. The geometries of the calorimeters are described in table 2. The number of radiation lengths (X_0) and interaction lengths are calculated from the table of the Particle Data Group [10]. The planes of diodes were inserted in the calorimeters in the orders illustrated; they were installed in different slots to study their identification efficiency versus depth in the calorimeter. The Ansaldo diodes were only installed in the uranium calorimeter, replacing the Micron diodes.

The calorimeters and diodes were mounted on a table which could be remotely controlled to move in the two directions transverse to the beam. The table and its control system could reproducibly locate the experiment to a precision of about 1 mm in each direction.

The experiment was located in the T7 unseparated test beam at the CERN PS. Data were taken at 3, 5 and

Table 1
Geometry of the diodes used in the experiment

Manufacturer	No.	Width [mm]	Height [mm]	Separation [mm]	Thickness [μm]
Hamamatsu	8	3.5	28.0	0.0	300
T.U. München	25	10.0	10.0	4.0	300
Micron	25	10.0	10.0	2.0	300
Ansaldo	21	10.0	10.0	2.0	400

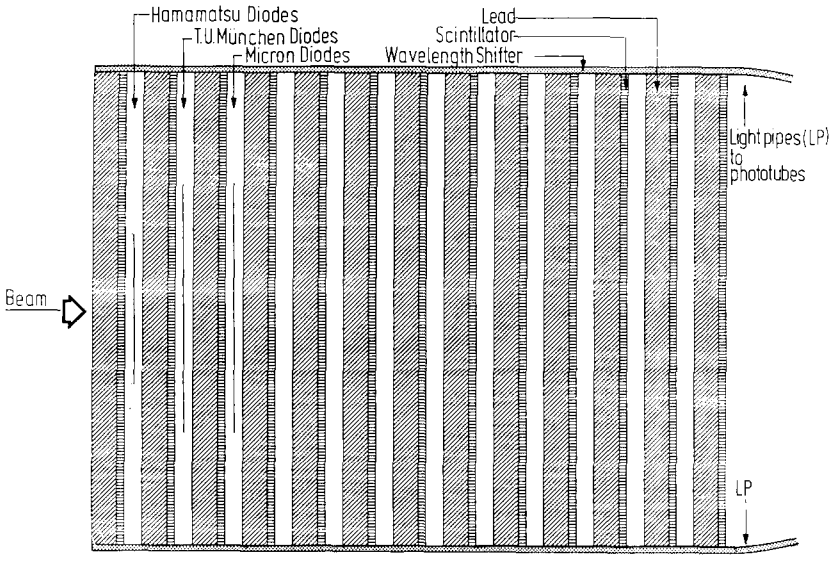

Fig. 2. Schematic diagram of the installation of the diode planes in the lead–scintillator calorimeter.

9 GeV. The layout is illustrated in fig. 4. A coincidence of the beam-defining counters, $B_1 \cdot B_2 \cdot B_3 \cdot \bar{B}_4$, was used to trigger the data acquisition system. Hadrons and electrons were then identified in the two Cherenkov counters, which were filled with CO_2 to the pressures listed in table 3.

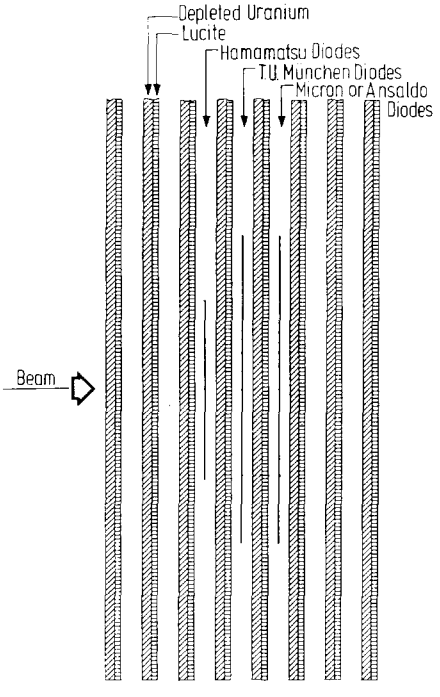

Fig. 3. Illustration of the installation of the diode planes in the stack of depleted uranium and Lucite.

Table 2
Parameters of the active lead–scintillator calorimeter and the simulated uranium–Lucite calorimeter

Properties	Calorimeter	
	Lead	Uranium
Plate thickness [mm]	10	3
Scintillator	Plastic	Lucite
Scintillator thickness [mm]	3	2
Slot thickness [mm]	7	7
Number of layers	13	8
Total length [mm]	260	96
Layer thickness (X_0)	1.8	0.94
Total thickness (X_0) (diodes are placed between 0 and $9X_0$)	23.4	7.5
Total thickness (λ_{int})	0.76	0.23

The pulse heights from the Cherenkov counters C_1 and C_2 and the muon counter, μ, were not included in the trigger, but were recorded on the data type for off-line analysis.

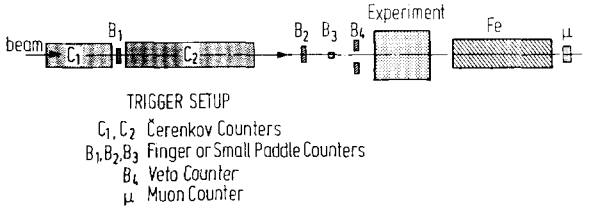

Fig. 4. Illustration of the beam line used in the text experiment. B_1 and B_2 are beam-defining paddle counters. B_3 is a small finger counter and B_4 is a veto counter with a 2.2 cm diameter hole for the beam.

Table 3
Absolute CO_2 pressures used in the two Cherenkov counters and the muon and pion thresholds

p [GeV]	Pressure [atm]	μ-threshold [atm]	π-threshold [atm]
3	0.6	1.51	2.64
5	0.6	0.54	0.95
9	0.3	0.17	0.29

The front-end electronics used [11] is illustrated in fig. 5. It was originally designed for the fast readout of microstrip detectors in the active target experiment NA 32 at CERN. It included 48 channels of:
- hybrid thick-film preamplifiers, MSD 2, with a trans-resistance gain of 10 mV/μA at a 50 Ω output load and an equivalent noise charge (ENC_{rms}) of 2100 electrons (e) with a 50 pF input capacitance;
- hybrid thick-film amplifier-line-drivers with a differential voltage gain of about 10 mV and a linear dynamic output range of ±450 mV, connected to the main amplifiers by 40 m twisted-pair cables with a damping factor of 2.2;
- main amplifiers on printed circuit boards, nominal gain of 10, linear output range of ±1 V, connected to the ADCs by 40 m twisted-pair cables;
- LeCroy 2282B ADCs used with 75 ns gate width.

The final output pulse had a length of 60 ns and a rise time of 10 ns. The total equivalent noise charge with a typical diode (Micron diode 6) connected was about 4600 e. The charge produced most probably by *one* minimum ionizing particle (mip) in a 300 μm thick diode – fully depleted up to 280 μm – is about 25 000 e and defines the mip signal. For one mip the signal-to-noise ratio is 5.4. The amplifier chain is linear up to signals of 20 mips; the gain drops 20% at 40 mips and 55% at 120 mips.

For calibration with minimum ionizing particles, the planes of diodes were placed in front of the calorimeter,

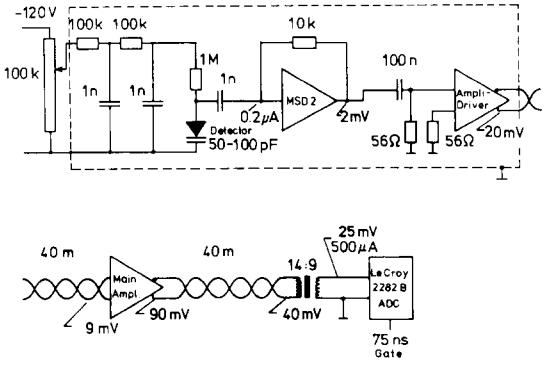

Fig. 5. Illustration of the electronics used. The quoted signal heights refer to a 1 mip signal.

Table 4
Measured composition of the test beam at the three momenta used in the experiment; the meanings of the columns are explained in the text

p [GeV]	f_h [%]	f_e [%]	f_μ [%]	f_{lost} [%]
3	56.3	35.9	0.7	7.1
5	78.1	16.6	2.4	2.9
9	86.6	3.1	7.5	2.8

and data were recorded in a scan in which the apparatus was moved so that the beam was centered on each of the diodes used in the experiment. The diodes were then installed in slots in the calorimeter and data were

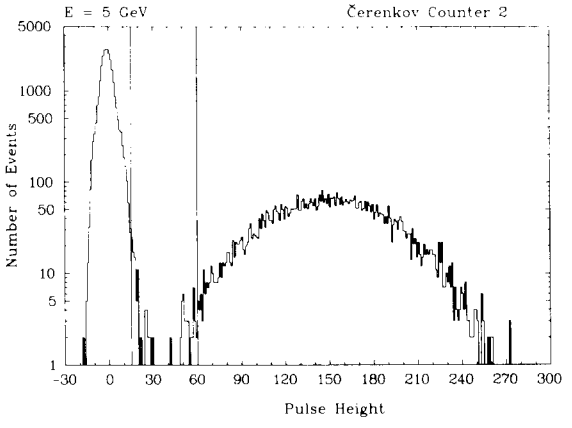

Fig. 6. The pulse height distributions in Cherenkov counter C_2 for the 5 GeV unseparated beam of hadrons and electrons. The vertical lines are the cuts used to identify hadrons and electrons in C_2.

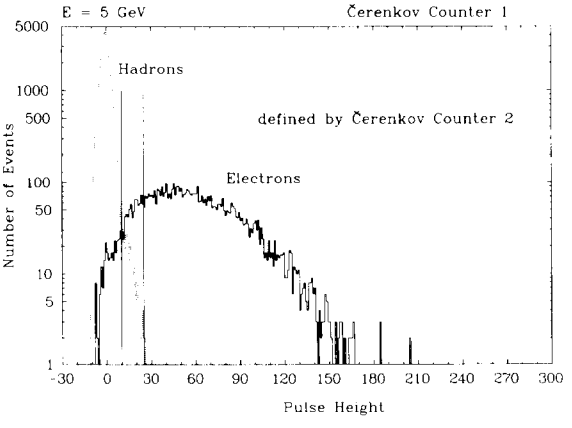

Fig. 7. The pulse height distribution in Cherenkov counter C_1 for 5 GeV particles identified as electrons in C_2 (solid line), and identified as hadrons in C_2 (dotted line). The vertical lines are the cuts used to separate hadrons and electrons in C_1.

then taken with the beam incident on the center of the 9 diodes marked in fig. 1. The beam was also directed at other transverse positions and the planes of diodes were moved to different depths in the calorimeter in order to cover the range of depths between $1X_0$ and $9X_0$. As the planes of diodes were moved to different depths in the calorimeter, a given slot was covered by diodes from the different manufacturers. Hence, any systematic differences in the performance of the different diodes could be detected. For the runs involving the simulated uranium calorimeter, the lead calorimeter was placed behind the uranium–plastic stack.

Since the purpose of this experiment is to study the efficiency of silicon diodes for e–h separation, clean identification of the incident particles is essential. Table 4 gives the measured compositions of the beam at 3 ,5 and 9 GeV, based on the analysis cuts described below. Particles detected in the μ-counter were eliminated from the data sample; the fraction of the incident particles eliminated by this cut is listed as f_μ in the table 4. Tight disjoint cuts for each of the two Cherenkov counters were used to identify hadrons and electrons; a particle was tagged as a h (e) only if it satisfied the h (e) cuts in both counters. Figs. 6 and 7 illustrate the Cherenkov counter pulse height distributions. The fractions of the incident beam particles identified as h or e are given in the columns labeled f_h and f_e, respectively, in table 4. Since the h and e cuts were disjoint, some particles were not identified as either h or e and were rejected; these appear in the column labeled f_{lost} in table 4.

The Cherenkov counters were very efficient for electrons at 3 and 5 GeV. At 9 GeV, the electron efficiency of C_1 was not as high. However, it can be demonstrated that, with the pulse height cuts applied, only one wrongly identified electron is expected in the sample of 18 000 selected hadrons. At 3 and 5 GeV the pressure used was well below the pion threshold; at 9 GeV the pressure was just above the pion threshold, but the efficiency for detecting pions was negligible. There was at most one wrongly detected hadron in the sample of 700 electrons.

For muons, the pressure was well below threshold at 3 GeV, just above threshold where the muon efficiency was small at 5 GeV, and well above the threshold at 9 GeV. f_μ is not a precise measure of the muon fraction

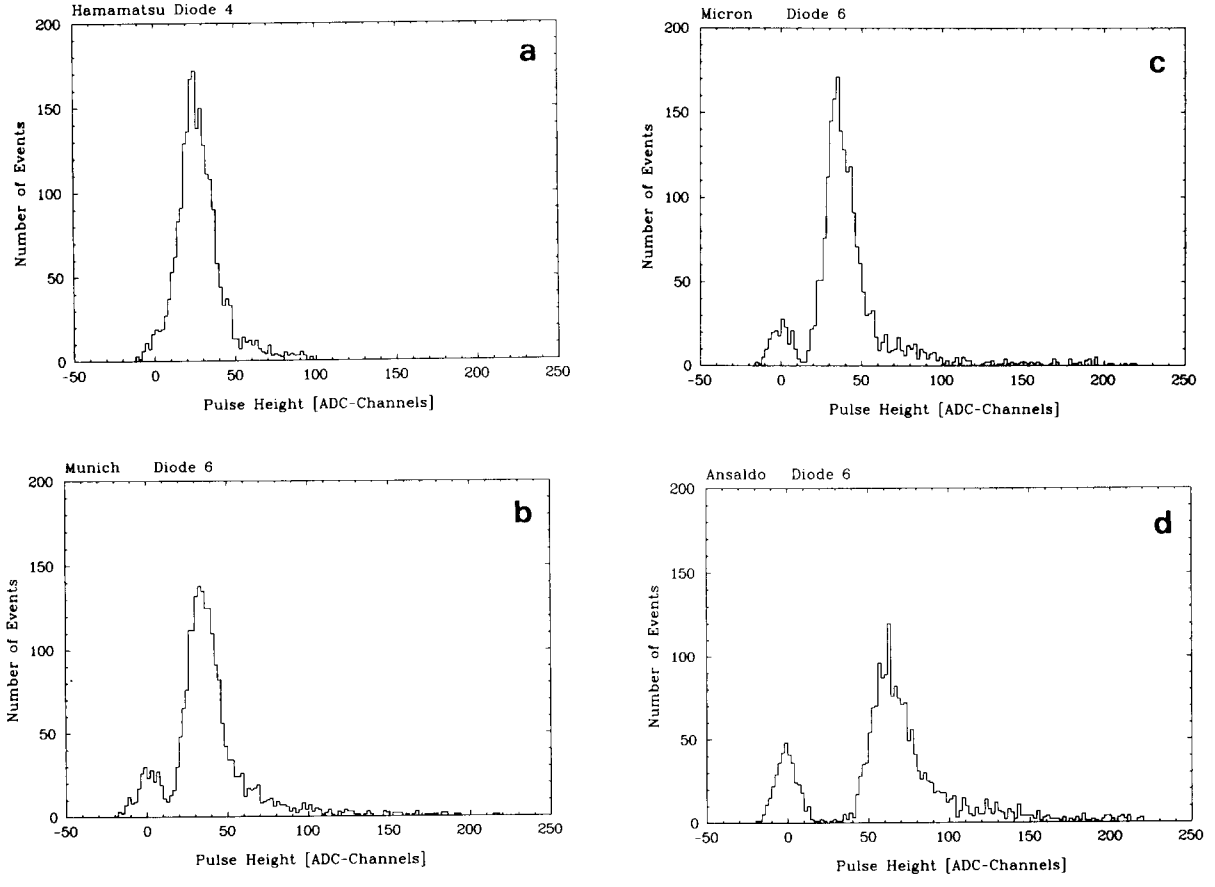

Fig. 8. Typical pulse height distributions for (a) Hamamatsu, (b) München, (c) Micron and (d) Ansaldo diodes for minimum ionizing particles. Some beam particles missed the diodes, which accounts for the small peak around 0.

in the beam due to the finite size of the muon counter and hadron punchthrough. Estimations indicate that the contamination of the h and e samples due to muons not detected in the μ-counter could be at most about 2% of the incident number of particles. At 3 and 5 GeV, any muons not counted in the μ-counter would be included in the hadron sample, where a muon contamination of this size would be negligible. This is due to the fact that muons would appear to be non-interacting hadrons and would be detected as minimum ionizing particles by the silicon diodes, where they would be a small correction to the large number of hadrons that were correctly identified by the diodes. At 9 GeV muons would have been included in the electron sample. The calorimeter pulse height spectrum for particles identified as electrons by the Cherenkov counters shows that this contribution is negligible.

If there were any remaining contamination of hadrons or muons in the electron sample or vice versa, the results presented here would underestimate the ability of solid state detectors to distinguish between h and e.

3. Results for one plane of diodes

From the scan with the diodes in front of the calorimeters we determined, for each diode, the most probable response to a minimum ionizing particle. In this way individual calibration factors (i.e. scale factors for the mip signals) were obtained for each diode.

Typical pulse height distributions of mips in individual diodes are shown in fig. 8 for Hamamatsu, München, Micron and Ansaldo diodes. In all cases the mip signals are well separated from the small pedestal peaks around zero pulse height which are due to the fact that some beam particles missed the sensitive area of the diode.

In the following we discuss the results with the diodes inside the calorimeter. In order to take into account the transverse width of particle showers in the silicon planes, the calibrated pulse heights of nine diodes of a square centrally hit by the beam were added in the off-line analysis (for the Hamamatsu diodes the signals in the eight strips were added). Fig. 9 shows the characteristic pulse height distributions in silicon pads for electrons (full line) and hadrons (dotted line) which, in this case, were obtained at a beam energy of 5 GeV in eight Hamamatsu diodes placed in the lead–scintillator setup behind $4.5X_0$. Most hadron signals are at low pulse heights, showing, however, a long but weakly populated tail toward higher pulse heights, whereas electrons peak at distinctly higher energies with an approximately Gaussian distribution.

Since all diode arrangements show, when placed at the same position in the stack, very similar distributions of the calibrated signals, we conclude that, for this experiment, the different arrangements can be considered as equivalent and interchangeable. Therefore, for the remainder of this article we will omit references to the type of diodes with which individual sets of measurements were performed.

e–h separation can be achieved by cuts in the pulse height recorded for the silicon planes. The fraction of electrons with a pulse height lower than the cut is defined as the electron inefficiency, and the fraction of hadrons with a pulse height higher than the cut is the

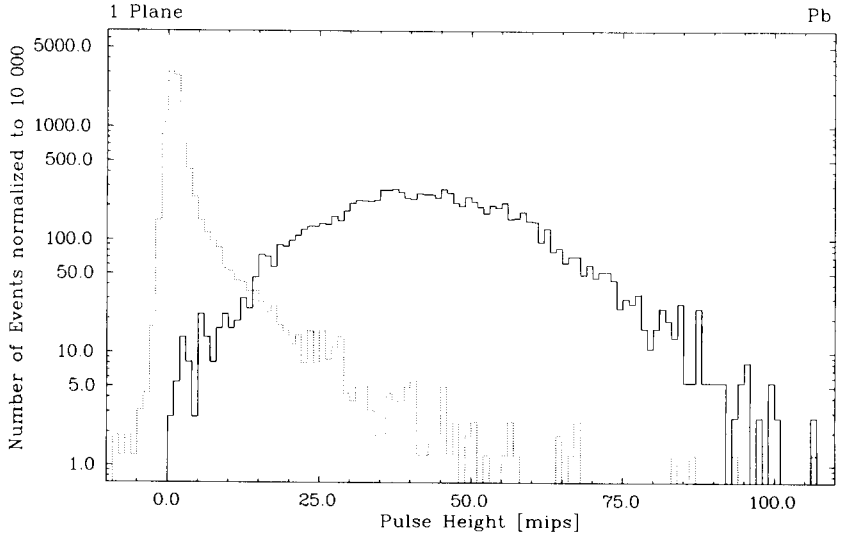

Fig. 9. Histograms of the pulse height distributions for 5 GeV particles identified as hadrons (dotted line) and electrons (solid line) by the Cherenkov counters. The diodes were at a depth of $4.5X_0$ in a lead–scintillator calorimeter. The two distributions are normalized to the same number of particles.

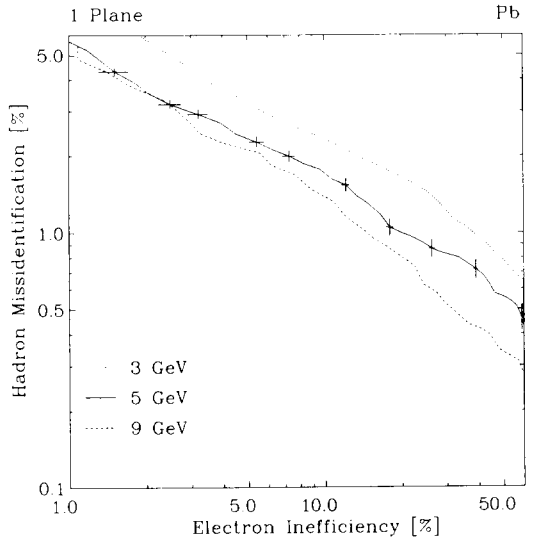

Fig. 10. Hadron misidentification probability versus electron inefficiency as obtained with one silicon plane for 3, 5 and 9 GeV particles. The diodes were at a depth of $4.5X_0$ in the lead–scintillator calorimeter. Errors indicated at a few points at 5 GeV are typical of all energies.

hadron misidentification probability. Clearly, higher pulse height cuts imply lower hadron misidentification and also lower electron efficiency.

Fig. 10 shows the hadron misidentification versus the electron inefficiency, with a single silicon plane placed at $4.5X_0$ in the lead calorimeter, for beam energies of 3, 5 and 9 GeV. At a fixed electron efficiency of 90% the corresponding hadron misidentification probabilities amount to:

- 2.6% at 3 GeV,
- 1.7% at 5 GeV,
- 1.5% at 9 GeV.

Since the curves in fig. 10 result from an integral distribution, the errors of nearly points are highly correlated. The errors are shown only for the measurement at 5 GeV; the other measurements have similar errors.

The improvement of hadron rejection with increasing energy is related to the growth of the electron showers, giving larger signals at higher energies and, therefore, better separation from the hadron-induced pulse heights.

The silicon plane position at $4.5X_0$ corresponds to the shower maximum for 5 GeV electrons. For this case we list in table 5 the hadron misidentification for various electron efficiencies.

The dependence of the e–h separation on the plane position in the stack is shown in fig. 11a for the lead calorimeter and in fig. 11b for the uranium–Lucite stack. The hadron misidentification at 90% electron efficiency is plotted as a function of the plane position in radiation lengths for the three beam energies. The

Table 5
Results from one plane of diodes after 4.5 radiation lengths at 5 GeV

Electron efficiency [%]	Hadron misidentification [%]
99	5.68 ± 0.18
95	2.35 ± 0.12
90	1.71 ± 0.10
80	0.99 ± 0.08

minimum of the curves moves slowly towards larger depths as the energy increases. We have verified by Monte Carlo simulation of the electromagnetic showers that the position of the minimum for a given energy agrees well with the shower maximum. The corresponding curves for other electron efficiencies (not shown) run roughly parallel to those in fig. 11 and, in particular, they have their minima at the same position.

Comparing the measurements in lead (fig. 11a) to those in uranium (fig. 11b), we conclude that the e–h separation in the two materials is quite comparable, possibly somewhat better in uranium. The relatively flat minima of the curves in fig. 11 will ensure that, for a given pad position, one obtains optimal e–h separation over a wide range of energies and that the rejection will hardly depend on the incident angle of the particles.

4. Results for two planes of diodes

Substantially improved e–h separation can be obtained using the correlation between the signals in two silicon layers placed at different depths in a calorimeter.

A correlation plot of the pulse heights from two planes of diodes in the lead calorimeter, one behind $3.6X_0$ and the other one behind $7.2X_0$, is shown in fig. 12 for electrons (a) and hadrons (b) at 5 GeV beam energy. Four different methods were tried to separate electrons from hadrons in the two-dimensional pulse height space: the curves in fig. 12 mark the boundaries between the electron and the hadron region as defined

Table 6
Results from two planes of diodes after $3.6X_0$ and $7.2X_0$ at 5 GeV (the errors given are typical statistical errors)

Electron Efficiency [%]	Hadron misidentification [%]				
	Rectangles	Ellipses	Circles	Hyperbolas	Errors
99	2.47	2.20	1.75	1.66	0.10
95	0.65	0.40	0.45	0.45	0.05
90	0.39	0.26	0.26	0.25	0.04
80	0.19	0.15	0.16	0.15	0.03

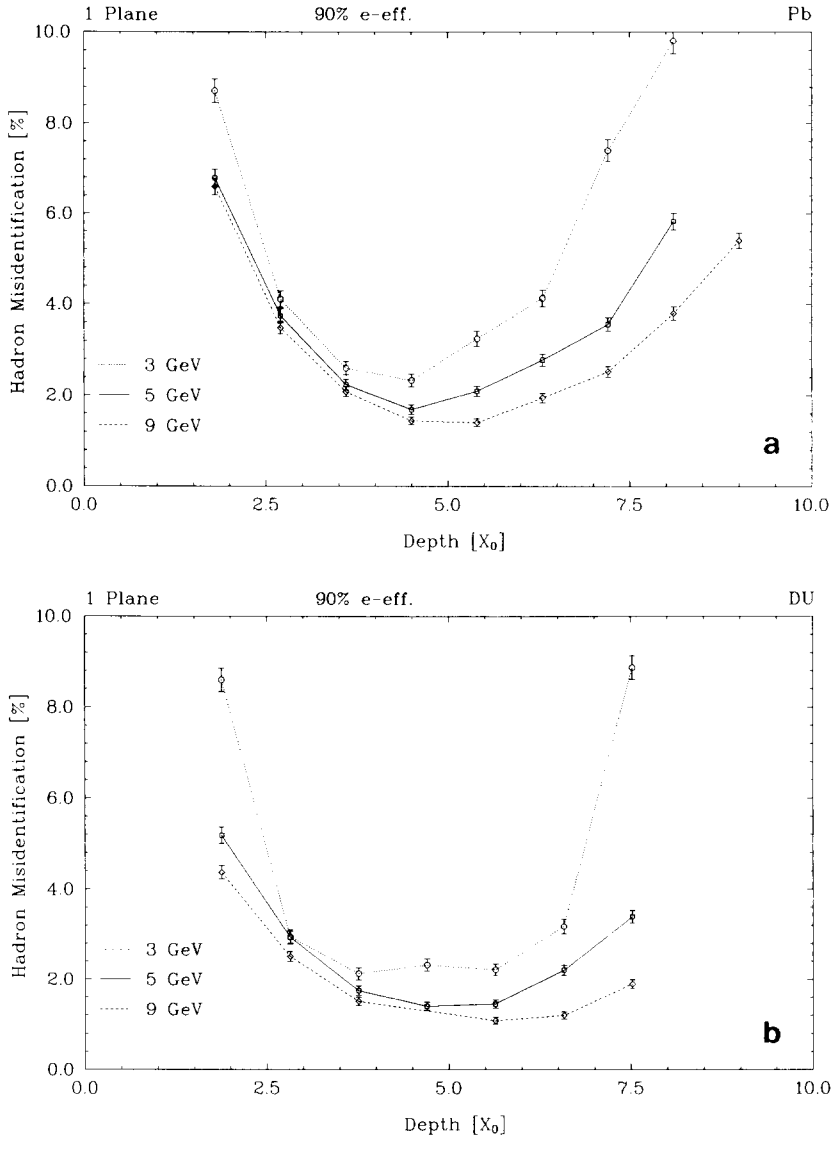

Fig. 11. Hadron misidentification versus depth at 90% electron efficiency for 3, 5 and 9 GeV particles. The diodes were in a lead–scintillator (a) and in a uranium–Lucite stack (b).

by these methods, for an electron efficiency of 90%. We briefly describe these separation methods.

- *Method 1 (ellipses)*
  The cut between the electron and hadron regions is performed along ellipses resulting as curves of equal probability density from a Gaussian approximation of the two-dimensional electron pulse height distribution. They are obtained by evaluating the bilinear and quadratic moments of the centered distribution. The low pulse height part of the ellipses is continued by a horizontal and a vertical tangent. The cut depends on one parameter, which is determined by fixing the electron efficiency.
- *Method 2 (rectangles)*
  A rectangle parallel to the axes is positioned in such a way that, for a given electron efficiency, the hadron misidentification is minimized. The method uses two free parameters (coordinates of the rectangle apex) which are determined in the minimization procedure.
- *Method 3 (circles)*
  The cuts are performed along a curve consisting of a circle around the point which marks the pulse height of one mip in two dimensions, and a horizontal and vertical straight line. Note that the circular part of the separation curve is concave when seen from the origin, whereas the elliptic cut is convex. This method

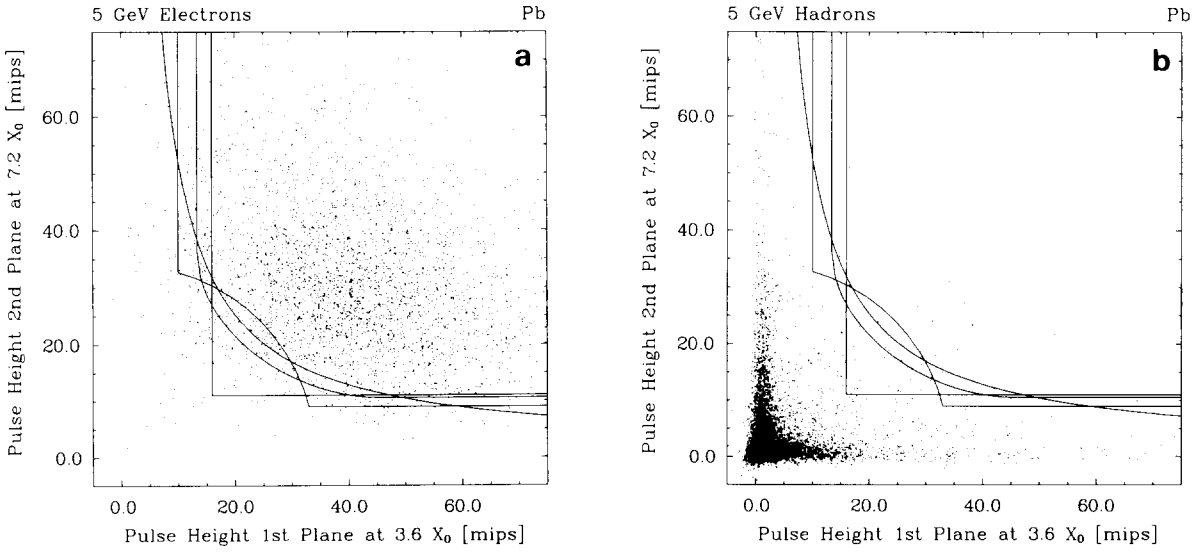

Fig. 12. Scatter plot of the signals in 2 silicon planes at $3.6X_0$ and $7.2X_0$ in a lead–scintillator calorimeter for electrons (a) and hadrons (b) at 5 GeV. The curves used for e–h separation correspond to an electron efficiency of 90%. The different curves are discussed in the text.

implies three free parameters (radius of circle and distances of straight lines from the axes) to be determined by the minimization.

- *Method 4 (hyperbolas)*

The cuts are performed along hyperbolas of the form $(x-1)(y-1)=s^2$ where the pulse heights x and y are assumed to be measured in units of mips. Thus s is the only parameter. This method is particularly convenient, since one may use the above hyperbola equal to define a "hyperbolic pulse height", s, for each pulse height pair, (x, y), and treat the whole problem as one-dimensional (this is a general feature of any set of curves defined by one parameter). Fig. 13 illustrates the hyperbolic pulse height for two layers at $3.6X_0$ and $7.2X_0$. Both the electron and hadron pulse height distributions are sharper than those for a single plane at either depth (compare to fig. 9). This illustrates directly the fact that two planes at different depths can separate hadrons and electrons more effectively than only one at either depth.

In table 6 we compare the hadron misidentification obtained with these methods for different electron efficiencies. The worst hadron rejection is obtained with

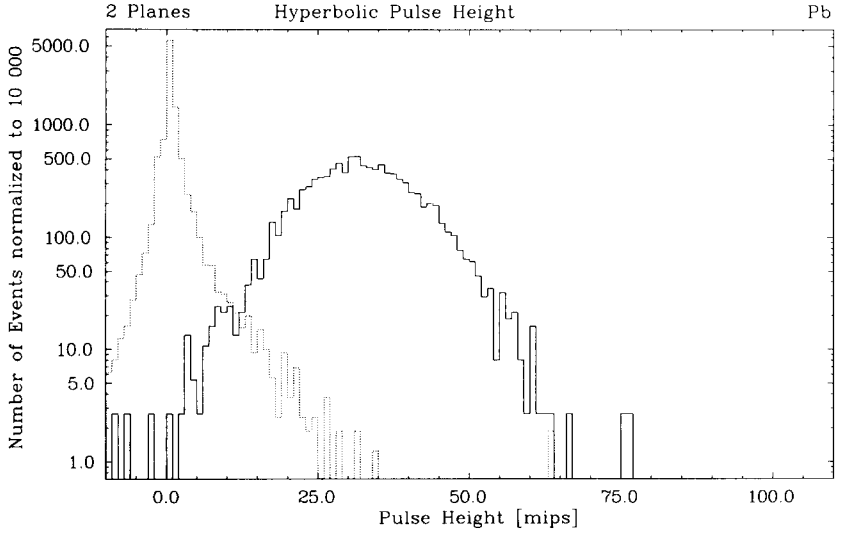

Fig. 13. Histogram of the hyperbolic pulse height in the same configuration of the previous picture.

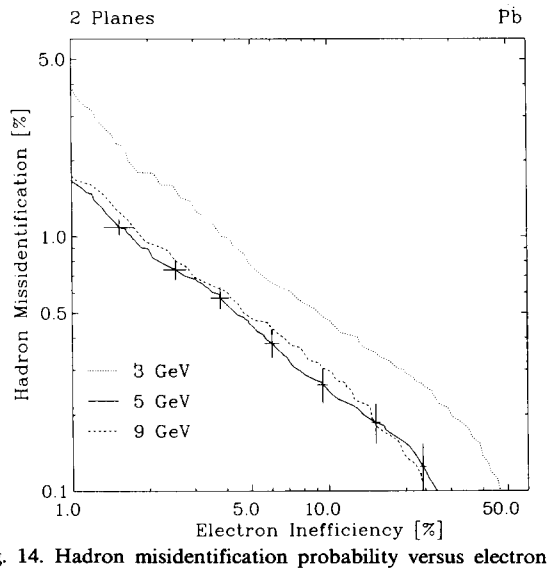

Fig. 14. Hadron misidentification probability versus electron inefficiency as obtained with two silicon planes at $3.6X_0$ and $7.2X_0$, for particle energies of 3, 5 and 9 GeV. The diodes were in the lead–scintillator calorimeter.

the rectangular cuts which penetrate too deeply into the hadron distribution, whereas the other three methods yield quite comparable results. The circular and hyperbolic cuts seem to have some advantages at very high (9%) electron efficiency where they are apparently more suitable boundaries of the hadron distribution than the other cuts.

In fig. 14 we have summarized our results on e–h separation at 3, 5 and 9 GeV with two silicon layers at $3.6X_0$ and $7.2X_0$ in the lead–scintillator calorimeter. The diode plane positions chosen correspond to near optimum separation in the energy range between 5 and 9 GeV. From the graphs in fig. 14 (obtained by the elliptic cut method) one reads at an electron efficiency of 90% the following hadron misidentifications:

- 0.5% at 3 GeV,
- 0.3% at 5 GeV,
- 0.3% at 9 GeV.

For the uranium the corresponding results are similar with somewhat better particle separation. Compared to a single silicon layer, a second layer gains an additional factor of about 6 in hadron rejection in the energy range studied.

Fig. 15 shows the influence of the distance in radiation lengths, Δx, between two silicon layers on the separation efficiency in the lead calorimeter. In each of the subfigures a, b and c which correspond to 3, 5 and 9 GeV, respectively, we plot the hadron misidentification at 90% electron efficiency as a function of the position of the first silicon layer for the two different layer separations studied in the experiment, namely $\Delta x = 1.8X_0$ and $\Delta x = 3.6X_0$. For all three energies better e–h separation is achieved for $\Delta x = 3.6X_0$, independent of the position of the first plane. The minimum of hadron misidentification moves from $2.7X_0$ for the position of the first plane at 3 GeV to $3.6X_0$ at 5 and 9 GeV, all with $\Delta x = 3.6X_0$. Furthermore, one observes that the difference between the hadron misidentifications ob-

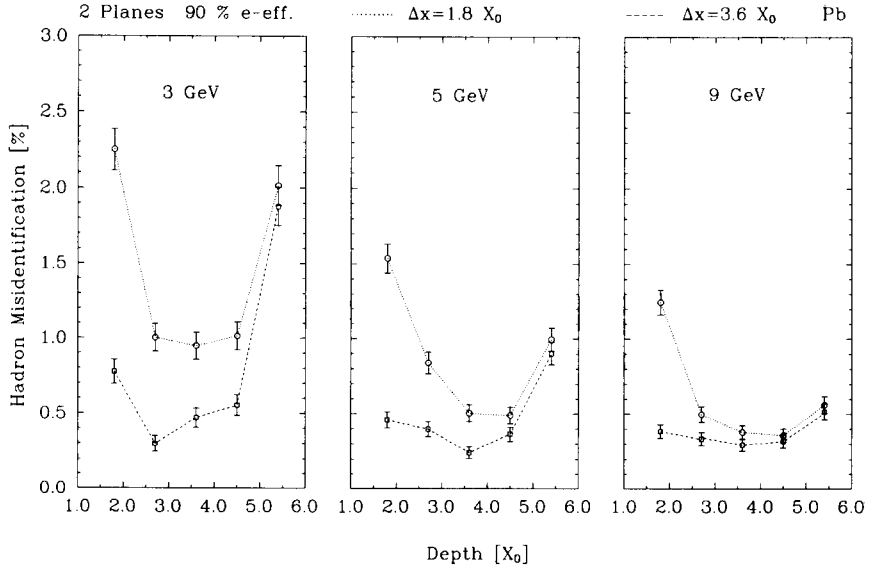

Fig. 15. Hadron misidentification probability versus depth of the first plane at 90% electron efficiency as obtained with two silicon planes separated by $1.8X_0$ and $3.6X_0$ for particle energies of (a) 3, (b) 5 and (c) 9 GeV. The diodes were in the lead–scintillator calorimeter.

tained with the two different Δx values decreases with increasing position depth of the first plane and with increasing energy of the particle. It is conceivable that greater distances between the planes could lead to better e–h separation, especially at higher energies. It was not possible to investigate this conjecture, given the beam energy and time constraints of the test experiment: data with additional separation Δx would have been required to find the best value.

5. Conclusions

The test results demonstrate that silicon layers, inserted at suitable depths in a sampling lead–scintillator or uranium–scintillator calorimeter, provide the additional information on the shower behaviour for e–h separation which in a poorly segmented calorimeter is needed to recognize electrons inside jets. In the energy range between 3 and 9 GeV a single detector plane provides a hadron rejection of 2% for 90% electron efficiency. A second plane improves the rejection by another factor 6. Given the fine segmentation, this detector provides good electron identification both for isolated electrons as well as electrons inside jets. Optimum positions for those detectors have been determined experimentally for one and two layers.

Acknowledgements

We wish to thank Dr. J. Kemmer who gave us the T.U. München diodes and Dr. P.G. Rancoita who furnished the diode fabricated by Ansaldo. We gratefully acknowledge the contributions of Prof. H. Brückmann, Dr. W. Vogel and Mr. U. Behrens to the construction and operation of the data acquisition system. We are indebted to Mr. K. Westphal and Mr. V. Sturm for their help in building the calorimeter and other mechanical structures used in the experiment. We are pleased to acknowledge the contributions of Mr. C. Ricci to the construction of the experiment and data taking at CERN. We appreciate the contributions of the CERN directorate and staff for their hospitality and assistance during our work at CERN.

References

[1] ZEUS Collaboration, The ZEUS Detector Technical Proposal, DESY, Hamburg (March 1986).
[2] G. Backenstoss, B.D. Hyams, G. Knop and U. Stierlin, Nucl. Instr. and Meth. 20 (1963) 295.
[3] C.W. Fabjan and T. Ludlam, Ann. Rev. Nucl. Part. Sci. 32 (1982) 335.
[4] J. Engler, Nucl. Instr. and Meth. A235 (1985) 301.
[5] For an introduction to semiconductor detectors and their use in high-energy physics see e.g. C.J.S. Damerell, Appleton Laboratory Report RAL-86-077, presented at the Advanced Study Institute on Techniques and Concepts of High Energy Physics, St. Croix, June 1986.
[6] For an introduction to calorimetry using silicon detectors and references to earlier work see e.g. P.G. Rancoita and A. Seidman, CERN-EP/86-113, presented at the 3rd Pisa Meeting on Advanced Detectors, Castiglione della Pescaia, 2–7 June 1986.
[7] Hamamatsu Photonics K.K., 1126-1 Ichino-cho, Hamamatsu City, Japan.
[8] Micron Semiconductor Limited, 1 Royal Buildings, Marlborough Road, Churchill Industrial Estate, Lancing, Sussex, BN15 8UN, UK.
[9] Ansaldo, Unità Semiconduttori, Via N. Lorenzi 8, 16152 Genova, Italy.
[10] Particle Data Group, M. Aguilar-Benitez et al., Phys. Lett. B170 (1986) 1.
[11] P. Jarron and M. Goyot, Nucl. Instr. and Meth. 226 (1984) 156.